SINGLE-PASS-AMPLIFIER FOR OPTICAL STOCHASTIC COOLING PROOF-OF-PRINCIPLE EXPERIMENT AT IOTA*

M.B. Andorf[1], V.A. Lebedev[2], P. Piot[1,2], and J. Ruan[2]
[1] Department of Physics and Northern Illinois Center for Accelerator & Detector Development, Northern Illinois University DeKalb, IL, USA
[2] Fermi National Accelerator Laboratory, Batavia, IL, USA

Abstract

Test design of a single-pass mid-infrared Cr:ZnSe optical amplifier for an optical stochastic cooling (OSC) proof-of-principle experiment foreseen at the Integrable Optics Test Accelerator (IOTA) ring part of Fermilab Accelerator Science & Technology (FAST) facility. We especially present an estimate of the gain and evaluate effects of thermal lensing. A conceptual design of the amplifier and associated optics is provided.

INTRODUCTION

Optical stochastic cooling is a promising technique to mitigate luminosity degradation in hadron colliders [1]. In OSC, the beam information is obtained via electromagnetic-radiation process (pick-up) and the required correction is applied by coupling back the amplified radiation to the beam (kicker). In Ref. [1] considered the use of pick-up and kicker quadrupole-wiggler magnets. The OSC was subsequently extended to enable cooling of beams with large initial emittances [2]. In the latter case, the pick-up and kicker are conventional dipole-type undulator magnets. The electron beam and undulator radiation are physically separated between the two undulators to permit amplification of the radiation and to delay the electron beam using a four-dipole chicane beam line. Fermilab is planning a proof-of-principle experiment of OSC in IOTA located at FAST [3]. The experiment will employ a 100-MeV electron beam so that sufficient undulator-radiation flux from the pick-up undulator reaches the kicker undulator with or without an optical amplifier (OA) to yield to an observable cooling effect.

The design of OA is considerably constrained. The longitudinal and transverse cooling ranges are respectively defined as $n_s = (\frac{\Delta P}{P})_{max}/\sigma_p$ and $n_x = \sqrt{(\epsilon_{max}/\epsilon)}$. Here P is the design momentum, σ_p is the rms momentum and ϵ is the horizontal beam emittance. $(\frac{\Delta P}{P}_{max})$ and ϵ_{max} represent boundaries for which particles that fall within will be cooled.

In case of equal damping rates in both planes it can be shown [4] that the cooling ranges reduce to

$$n_s \approx \frac{\mu_{01}}{\sigma_P k \Delta S}, \qquad n_x \approx \frac{\mu_{01}}{2k\Delta S}\sqrt{\frac{D^{*2}}{\epsilon\beta^*}}, \tag{1}$$

with $\mu_{01} \approx 2.405$ being the first zero of the Bessel function, $k = 2\pi/\lambda$ the wavenumber of the radiation (determined by the wavelength λ of the OA), ΔS is the electron-beam path-length delay introduce by the chicane and sets the optical delay of the OA system, and D^* and β^* are the respectively the dispersion and beta functions at the center of the chicane. From Eq. (1) we note that a longer operating wavelength for the OA allows for a larger delay and thus a longer crystal (resulting in a higher gain). A review of the available lasing media prompted us to choose Cr:ZnSe as our gain medium (center wavelength of $\lambda \simeq 2.49\,\mu$m) resulting in a delay ΔS of a few millimeters.

Previous OA designs for OSC were based on Ti:Sp ($\lambda \simeq 0.8\,\mu$m) as the gain medium [5, 6] because of its excellent bandwidth (95 THz FWHM [7]) and ability to produce high gain. Cooling rate is inversely proportional to the amplifier bandwidth and for Cr:ZnSe it is just 50 THz [8]. However to keep the same cooling range Eq. (1) indicates a Ti:Sp crystal would need to be 0.6 the length of a Cr:ZnSe crystal [the signal delay of an amplifier with a crystal of length L and index of refraction n is given as $\Delta S = L(n-1)$]. Furthermore even if both crystals could have the same delay it was shown in Ref. [9] that Cr:ZnSe is expected to produce superior gain at lower pump intensities.

Another advance of Cr:ZnSe is the large number of pumping options in the mid-IR range. Therefore we investigated how the pumping wavelength will affect the amplifier performances. Optical parametric amplification has been ruled out as it would require pulses long enough to cover the length of a bunch in IOTA (~ 14 cm corresponding to 470-ps duration) at a repetition rate of 7.5 MHz. Instead we concentrate on the design of a single-pass amplifier with CW pumping.

GAIN EQUATIONS

In this section we demonstrate how to calculate the gain of a signal passing through a pumped medium. We start with the population rate equation for a 4-level system. Let N_0 be the population density of the ground state and N_i, $i = 1, 2, 3$ be population densities of the excited states. If we only allow for spontaneous emission to occur between nearest energy levels the rate equations are given as

$$\frac{dN_3}{dt} = -\kappa_3 N_3 - \frac{\sigma_{pa} I_p}{h\nu_p}(N_3 - N_0), \tag{2}$$

$$\frac{dN_2}{dt} = \kappa_3 N_3 - \kappa_2 N_2 - \frac{\sigma_s I_s}{h\nu_s}(N_2 - N_1) - \frac{\sigma_{pe} I_p}{h\nu_p}(N_2 - N_0), \tag{3}$$

* Work supported by the by the US Department of Energy (DOE) contract DE-SC0013761 to Northern Illinois University. Fermilab is operated by the Fermi research alliance LLC under US DOE contract DE-AC02-07CH11359.

ISBN 978-3-95450-174-8

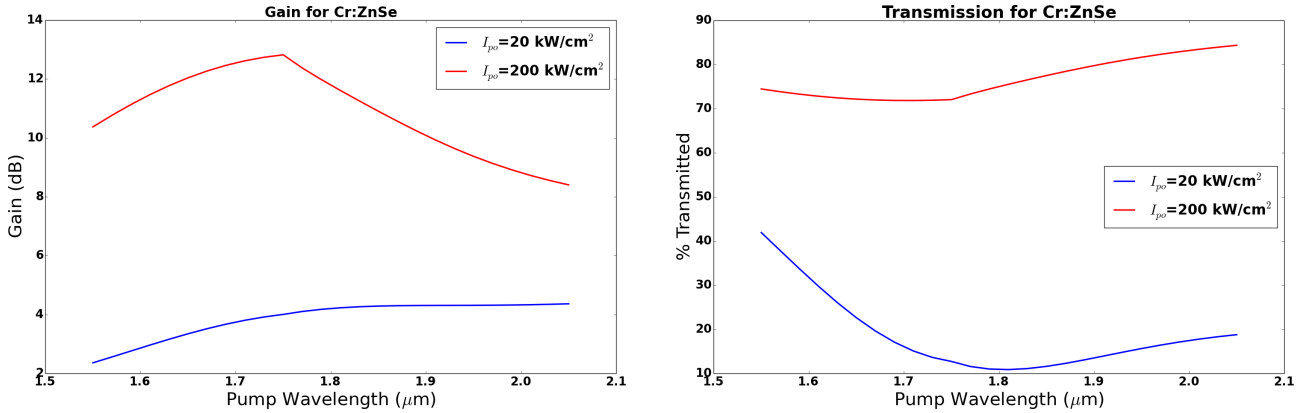

Figure 1: Left: Gain dependence on frequency for I_{po} 20 kW/cm^2 (blue) and 200 kW/cm^2 (red). Right: Corresponding transmission for both intensities as a function of wavelength.

$$\frac{dN_1}{dt} = \kappa_2 N_2 - \kappa_1 N_1 + \frac{\sigma_s I_s}{h\nu_s}(N_2 - N_1), \quad (4)$$

$$\frac{dN_0}{dt} = \kappa_1 N_1 + \frac{\sigma_{pa} I_p}{h\nu_p}(N_3 - N_0) + \frac{\sigma_{pe} I_p}{h\nu_p}(N_2 - N_0). \quad (5)$$

In the above, $\kappa_i = 1/\tau_i$ is the spontaneous decay constant (τ is the decay time), h is Planck's constant, ν is the photon frequency, σ is the frequency-dependent cross section, and I is intensity. The subscript s is for the signal (undulator radiation) to be amplified and the subscript p is for the pump laser. We further denote the cross sections of the pump with 'pa' for pump absorption and 'pe' for pump emission. This is specifically important for Cr:ZnSe because the corresponding absorption and emission cross sections overlap for wavelengths > 1.75 µm [8].

Attenuation of the pump laser intensity I_p as it propagates a distance z through the gain medium is given by

$$\frac{dI_p}{dz} = -I_p[\sigma_{pa}(N_0 - N_3) + \sigma_{pe}(N_0 - N_2)], \quad (6)$$

and growth of the signal intensity I_s is

$$\frac{dI_s}{dz} = I_s \sigma_s (N_2 - N_1). \quad (7)$$

The spontaneous decay rates of the first and third levels are prompt so that for a steady state $N_0 \gg N_3$ and $N_2 \gg N_1$ and Eq. (4) is approximated as $N_3 \simeq \frac{I_p \sigma_{pa} N_0}{h\nu_p \kappa_3}$ which in turn can be used to eliminate N_3 and κ_3 from Eq. (3).

The undulator radiation at the crystal entrance, I_{so} will be on the order of mW/cm^2. This is too small to affect the population dynamics and so stimulated emission due to undulator radiation is neglected in the rate equations. Using these simplifications with Eqs. (3), (6) and (7) yields

$$\frac{dI_s}{dz} = -\sigma_s A \frac{dI_p}{dz}, \quad (8)$$

with $A \equiv \frac{\tau_2}{h\nu_p}$. Defining the amplifier gain as $G = I_s/I_{so}$ the above equation is solved to give

$$G = e^{\sigma_s A (I_{po} - I_p)} \quad (9)$$

To calculate G the pump intensity dependence along the crystal must be known. To find this we first note that since $N_0 \gg N_3$ and $N_2 \gg N_1$ that the total doping concentration $N_t \approx N_0 + N_2$. This can be used to eliminate N_2 from Eq. (3) and (6). After substituting use Eq. (3) to solve for N_0

$$N_0 = \frac{N_t(1 + I_p \sigma_{pe} A)}{I_p A(\sigma_{pa} + 2\sigma_{pe}) + 1} \quad (10)$$

Finally we put the expression for N_0 into Eq. (6) to get

$$\frac{dI_p}{dz} = -I_p N_t \left(\frac{(1 + I_p \sigma_{pe} A)(\sigma_{pa} + 2\sigma_{pe})}{I_p A(\sigma_{pa} + 2\sigma_{pe}) + 1} - \sigma_{pe} \right) \quad (11)$$

Equation (11) can be integrated numerically. Equation (9) can then be used to study the gain dependence on various parameters such as the crystal length, doping concentration, and the frequencies of the signal and pumping laser (including both the explicit frequency dependence but also the implicit frequency dependence of the cross sections).

Figure 1 gives the dependence of the amplifier gain as a function of wavelength for two different initial pump intensities of $I_{po} = 200$ kW/cm^2 and $I_{po} = 20$ kW/cm^2 respectively refer to as "low" and "high" intensities cases. For both intensities the crystal parameters are identical and fixed to a doping concentration of $N_t = 2.0 \times 10^{19}$ ion/cm^3 and length $L = 1.4$ mm resulting in a signal optical delay of 2 mm.

σ_{pa} was approximated as a Lorentzian with a peak of 1.05×10^{-18} cm^2 at 1.78 µm and FWHM of 0.4 µm. σ_{pe} was treated as a continuous piece-wise function with $\sigma_{pe} = 0$ for wavelengths less than 1.75 µm and from 1.75 to 2.05 µm a straigh line with a slope of 2.5×10^{-18} cm^2/µm and an intercept of -4.36×10^{-18} cm^2. σ_s was kept constant at 1.2×10^{-18}cm^2 corresponding to the emission peak of Cr:ZnSe, 2.49 µm.

At high intensities the amplifier gain reaches its maximum at 1.78 µm where $\Delta I_p = I_p(z = 0) - I_p(z = L)$ is maximized. Although the absorption cross section is well approximated by a symmetric Lorentzian distribution, the gain appears asymmetric because of the overlap between absorption and emission cross sections at wavelengths below 1.75 µm, a region where the pump begins to self-stimulate. This latter

ISBN 978-3-95450-174-8

feature, along with a depleted ground state from the high intensity, renders the crystal very transparent at wavelengths above 1.75 µm.

At lower pump intensities the effect of self-stimulation is small. Rather for low intensities larger wavelengths lead to a slight increase of the gain at wavelengths past the absorption peak were ΔI is decreasing. This rise in the gain at larger wavelengths comes from the reduction in absorbed intensity that goes into heat, $I_h = \Delta I_p(1 - \frac{\lambda_p}{\lambda_s})$. The transmission as a function of wavelength is shown in the right side of Fig. 1.

For the case when $\sigma_{pe} = 0$, Eq. (11) can be solved in terms of the Lambert function $W(z)$, defined as the solution of $z = W(z)\exp[W(z)]$, and a closed-form solution for the gain can be obtained by expliciting

$$I_p = I_{sat} W\left(\frac{I_{po}}{I_{sat}} e^{-\alpha T + \frac{I_{po}}{I_{sat}}}\right) \tag{12}$$

into Eq. (9). In Eq. (12). we define $\alpha \equiv N_t \sigma_{pa}$ and $I_{sat} \equiv \frac{h\nu_p}{\sigma_{pa}\tau_2}$.

THERMAL LENSING

Cr:ZnSe is expected to have considerable thermal lensing due to the relatively high temperature dependence of the index of refraction and the high pumping intensities needed for the desired gain. The pump will have a flat top transverse distribution to help manage the lensing. For a cylindrical crystal with its surface temperature fixed and a uniform power distribution the focal length is given as [10]

$$f = \frac{\kappa A}{P_h}\left(\frac{1}{2}\frac{dn}{dT}\right)^{-1} = \frac{\kappa}{I_h}\left(\frac{1}{2}\frac{dn}{dT}\right)^{-1}, \tag{13}$$

with $\kappa = 1$ W/cm-K for cryogenically cooled Cr:ZnSe [11], and A is the transverse spot size. Figure 2 shows thermal lensing for high intensity. The increase in lensing with increased wavelength is again associated with an increase in transparency and a decrease in the fraction of absorbed intensity going to heat.

Another contribution to thermal lensing comes from the bulging of the flat faces of the crystal. The associated focal length is $f_b = \frac{\kappa}{I_h}\frac{\alpha r_o(n_o-1)}{L}$ [10] with $n_o = 2.44$, $\alpha = 7.3 \times 10^{-6}$ K^{-1} [12] being the expansion coefficient and r_o the pump spot size. For example using the high intensity and crystal parameters from the previous section a Thulium laser at 1.93 µm with $r_o = 100$ µm would result in a $f_b = 160$ cm. Therefore bulging has a minor contribution to the overall thermal lensing.

PUMP LASER SELECTION

Now that the effects of the pump wavelength laser are well understood we can select the most appropriate one. We consider two choices an Erbium laser at 1.55 µm and a Thulium laser at 1.93 µm. Both lasers can be bought off the shelf with at least 60 W of pump power. We note that both lasers have similar gain (as inferred from Fig. 1) with Erbium and Thulium matched at high intensity and Thulium performing better at low intensities.

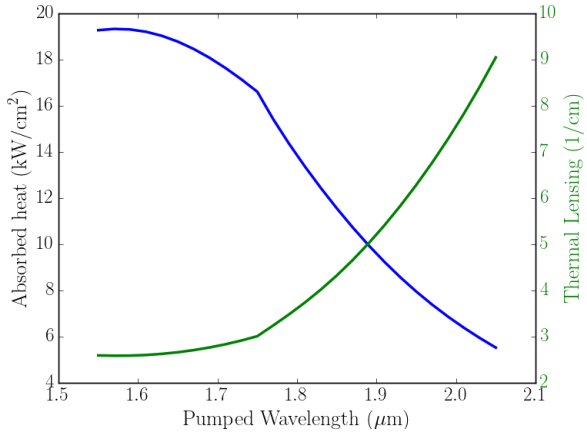

Figure 2: Thermal lensing (blue) and associated absorbed heat (green) evolution as a function of pump-laser wavelength. Both plots use the pump intensity $I_{po} = 200$ kW/cm^2.

It is clear that for optimal gain the crystal must be pumped as intensely as possible and given the high power available from these lasers this means pumping near the damage threshold is possible. Calculating the damage threshold is complicated as it depends on many factors, but generally it will decrease with decreasing wavelength [10] and from Figure 2 we see this is probably due to increasing absorbed heat at a fixed intensity. At 1.93 µm the absorbed heat drops by more than a factor of 2 thereby favoring the Thulium laser to pump at a higher intensity than the Erbium.

OPTICS

Beyond just the gain medium the OA requires some optics to accomplish three things (*i*) focus the pump laser to the required size at the crystal for desired intensity, (*ii*) focus the radiation from the pick-up undulator within the pump spot size at the crystal, and (*iii*) focus radiation originating from a certain longitudinal position in the pick-up to the corresponding point in the kicker. The latter of these requirements is accomplished by having the transfer matrix from pick-up to kicker center be $\pm\mathbf{I}$, the identity matrix [4].

In order to investigate possible optics designs we carried out a numerical simulation of the undulator radiation using the synchrotron radiation workshop SRW [13]. The radiation electric-field $\mathbf{E}(\mathbf{x})$ components are recorded on a transverse plane [$\mathbf{x} = (x, y)$] downstream of the undulator exit. In our convention the undulator radiation is polarized along the $\hat{x}$ direction so that the corresponding Wigner function is computed from the field component $E_x(\mathbf{x})$ following

$$\mathcal{W}_x(x, k_x) = \frac{1}{\lambda^2}\int_{-\infty}^{+\infty} E_x\left(x - \frac{x'}{2}\right) E_x\left(x + \frac{x'}{2}\right) \times e^{ik_x x'} dx', \tag{14}$$

where k_x the horizontal component of the wavevector and λ the radiation wavelength. Equation (14) can be rewritten for the vertical axis doing the substitution $x \leftrightarrow y$. Figure 3 shows a typical Wigner function produced by the undulator

ISBN 978-3-95450-174-8

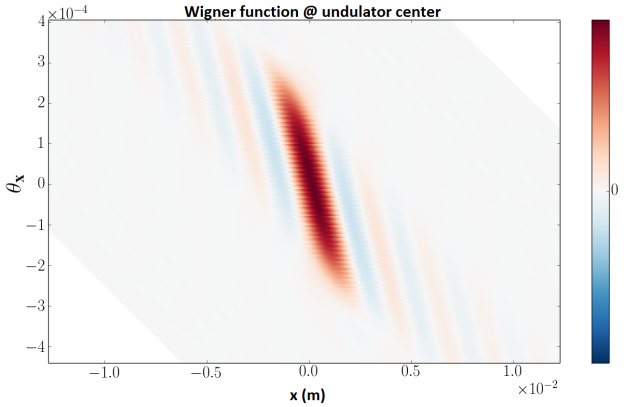

Figure 3: Example of Wigner function associated to the undulator radiation produced by a single electron; see Tab. 1 for the corresponding parameters. The Wigner function is back-propagated at the undulator center.

with parameters gathered in Table 1. A statistical analysis of the Wigner function provides the Courant-Snyder parameters of the photon beam that can be used as initial conditions for the optical design. Figure 4 shows a generic four-lens

Table 1: Undulator and Electron Parameters Used in the Optical Transport Design

Beam Energy	100 MeV
Undulator Period	12.9 cm
Number of Periods	6
Peak Magnetic Field	664 G
Zero angle wavelength	2.2 µm

setup. A simpler system incorporating two symmetric lenses only resulted in a spot radius on the crystal of $\approx 600\,\mu$m (assuming $f = 5$ cm from thermal lensing). The latter design would require a pump laser of 2300 watts for $I_{po} = 200$ kW/cm^2 which is unrealistic. Adding two more lenses reduces the radiation spot size on the crystal thereby relaxing the requirement on the pump-laser power. For the entire transfer matrix to be described by a unity matrix we require $D_1 = D_3$, $D_2 = D_4$ and $f_1 = (D_1 + D_2)/2$; see Fig. 4. The drifts D_1 and D_4 must be long enough to respectively be downstream and upstream of the first and last dipoles of the chicane. In our analysis we further consider the case $D_1 = D_4$ which results in the requirement $D_3 = D_2$. With the outer drifts chosen we find $L_1 = \sqrt{2fK}$, $F = \frac{LL_1}{K}$, $L = K/2 - L_1$ where $K \equiv (L_t - 4D_1)/2$ with $L_t = 3.3$ m being the total distance between the undulator centers. The additional lenses results in a spot size at the crystal of 100 µm thereby relaxing the laser power to $\sim$ 60 W. Considering the crystal discussed in the previous section pumped by a Thulium laser would result in 13 W of absorbed power with 3 W deposited as heat.

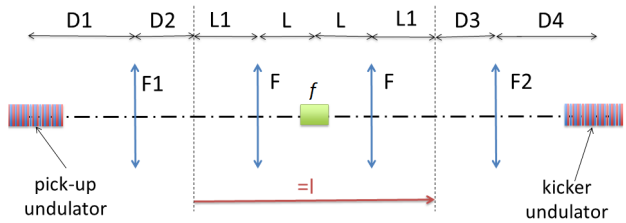

Figure 4: Optical system used to collect and transport the pick-up undulator radiation up to the kicker undulator. The double-arrowed lines represent optical lenses (Fn are the associated focal lengths).

FUTURE WORK

A potential limitation that needs to be investigated is the potential phase distortions occurring during amplification. Because the corrective kick a particle receives depends on the phase of the electromagnetic wave, this effect can impact the cooling performances. This effect will be quantify via an interferometry experiment. For a bench test an optical parametric amplifier will be built to mimic the large broadband of the undulator radiation. We must also investigate and minimize dispersion that will occur from the optics as this again impacts the phase of the electromagnetic wave. The chance for near zero dispersion exist because dispersion for Cr:ZnSe has the opposite dependence of most glass used for lenses in the mid-IR spectrum.

REFERENCES

[1] A.A. Mikhailichkenko, M.S. Zolotorev, Phys. Rev. Lett. **71** (25), p. 4146 (1993).

[2] M.S. Zolotorev, A.A. Zholents, Phys. Rev. E, **f50** (4), p. 3087 (1994).

[3] S. Nagaitsev et al., Proc. IPAC'12, New Orleans LA USA, p. 106 (2012).

[4] V.A. Lebedev, "Optical Stochastic Cooling," ICFA Beam Dyn.Newslett. **65** pp. 100-116 (2014).

[5] V.A. Lebedev et al., Proc. NAPAC'13 Pasadena, CA, USA, p. 422 (2013)

[6] A. Zholents, M. Zolotorev. Proc. PAC'97, Vancouver, B.C. Canada, p. 1805 (1998).

[7] Titan CW CW Ti:Sapphire Laser Operation Manual. Q-Peak Inc.

[8] Tm:ZnSe /S Series Data sheet available from IPG Photonics Inc. (2012).

[9] M.B. Andorf et al., Proc. IPAC'15, Richmond, VA, p. 659 (2015).

[10] W. Kochner, *Solid-State Laser Engineering*, 5th ed. Springer (1999).

[11] G. Slack, Phys. Rev. B 6, (10), p.3791, (1972).

[12] I.T. Sorokina, Opt. Mat. **26**, pp.395-412, (2004).

[13] O. Chubar, P. Elleaume, Proc. EPAC98, Stockholm Sweden, p.1177 (1998).

ISBN 978-3-95450-174-8